www.atmia.put.poznan.pl AMTM vol. 36 (2016) 18-22

Archives of Mechanical Technology and Materials

The influence of laser re-melting on microstructure and hardness of gas-nitrided steel

Dominika Panfil[a], Piotr Wach[b], Michał Kulka[a*], Jerzy Michalski[b]

[a] *Poznan University of Technology, Piotrowo 3 Street, 60-965 Poznan, Poland*

[a] *Institute of Precision Mechanics, Warsaw, Poland*

e-mail address: michal.kulka@put.poznan.pl

A B S T R A C T

In this paper, modification of nitrided layer by laser re-melting was presented. The nitriding process has many advantageous properties. Controlled gas nitriding was carried out on 42CrMo4 steel. As a consequence of this process, ε+γ' compound zone and diffusion zone were produced at the surface. Next, the nitrided layer was laser re-melted using TRUMPF TLF 2600 Turbo CO_2 laser. Laser tracks were arranged as single tracks with the use of various laser beam powers (P), ranging from 0.39 to 1.04 kW. The effects of laser beam power on the microstructure, dimensions of laser tracks and hardness profiles were analyzed. Laser treatment caused the decomposition of continuous compound zone at the surface and an increase in hardness of previously nitrided layer because of the appearance of martensite in re-melted and heat-affected zones.

Key words: gas nitriding, laser heat treatment, microstruture, hardness.

1. INTRODUCTION

Nitriding is one of the widely used surface treatment modifications, and it is very popular surface engineering method for improving the hardness and wear resistance. There are several methods of nitriding, e.g. controlled gas nitriding [1, 2], plasma nitriding [7-10] and salt bath nitriding [5].

Recently, the controlled gas nitriding was intensively developed. This process enables the control and regulation of the growth of the nitrided layer on steel by a nitriding potential value. The microstructure could be composed of ε+(ε+γ') iron nitrides with a predominant percentage of ε phase, ε+γ' iron nitrides, with a lesser percentage of ε phase and only γ' iron nitrides at the surface [3,4]. Compound zone (with nitrides) determined hardness close to the surface. The lower hardness was obtained when a porous ε iron nitrides appeared on the surface [3]. Hence, controlled gas nitriding was attractive because of the possibility of control of the phase composition at the surface and because of the repeatability of the phase composition at specified nitriding parameters.

The calculated hardness of iron nitrides was presented in the paper [6]. First principles of calculations were formulated to investigate hardness of ε-Fe_3N and γ'-Fe_4N phases. The hardness of the iron nitrides ε-Fe_3N was 9.48 GPa, whereas the hardness of γ'-Fe_4N phase was lower, obtaining 6.01 GPa. Strong Fe–N bonds were found to play important role in the hardness of these iron nitrides. Hardness depended on the method of nitriding but also on the substrate material, in which various phases were produced.

Surface modification by plasma nitriding was also a well-known process. This technique as an effective and simple method was widely used to improve the surface hardness [7, 13-14]. During the plasma nitriding, nitrogen diffused into the surface of the material where it connected to the substrate, with iron and alloying elements [15]. The produced nitrides strengthened the surface and caused compressive stresses in the surface layer. Nitride layer (compound zone) was relatively hard, but had a high state of internal stress, which frequently caused spalling and flaking of the nitride layer. When carbon steel was the substrate, the compound zone consisted mainly of iron nitrides, achieving a hardness of about 900 HV. In the case of plasma-nitrided stainless steel, chromium nitrides were also produced. Such a compound zone was characterized by the increased hardness up to about 1150 HV [7]. The surface hardness of aluminium and its alloys was also improved by plasma nitriding [8-9]. The formation of a hard AlN phase provided the hardness of 1600-1700 HV [8]. Plasma nitriding proved to be one of the most effective methods that improved the tribological properties of titanium and its alloys. During the plasma nitriding of titanium and its alloys, it was possible to produce a compound layer, containing δ-TiN and ε-Ti_2N phases with a hardness of about 1500-3000 HV [16,17]. Plasma nitriding was used to improve the surface hardness of Ti_2AlC soft ceramic with a relatively low hardness of about 3 GPa. After

plasma nitriding, hardness of this ceramic increased to 4.4 GPa [10].

Laser heat treatment (LHT) was also widely used to modify the previously nitrided steel [11,12]. With this modification, it was possible to increase the hardness of the surface, and increase in the depth of hardened zone.

In this study, the controlled gas nitriding process was followed by such a laser heat treatment. The influence of LHT parameters on the microstructure and hardness of laser-modified nitrided layer was studied.

2. EXPERIMENTAL PROCEDURE

In this study 42CrMo4 steel was used as material of the specimens. The composition of this steel was 0.38-0.45% C, 0.9-1.2% Cr and 0.15-0.25% Mo. The specimens were ring-shaped with an external diameter of 20 mm, internal diameter of 12 mm and a length of 12 mm. Before nitriding, the specimens were austenitized at 860°C (1123 K), quenched in oil and high-temperature tempered at 600°C (873 K).

Controlled gas nitriding was carried out in the atmosphere, consisting of ammonia. The process parameters were as follows: temperature 570°C (843K), time 4 h, the changeable nitriding potential. During the process of controlled nitriding, the selection of nitriding potential was very important, because of its influence on the microstructure of the nitrided layer. Nitriding potential was decreased vs. time of the process (**Figure 1**), ranged from its very high initial value to the intermediate value of 5 and finally to value 2 in order to reduce the thickness of the porous ε phase.

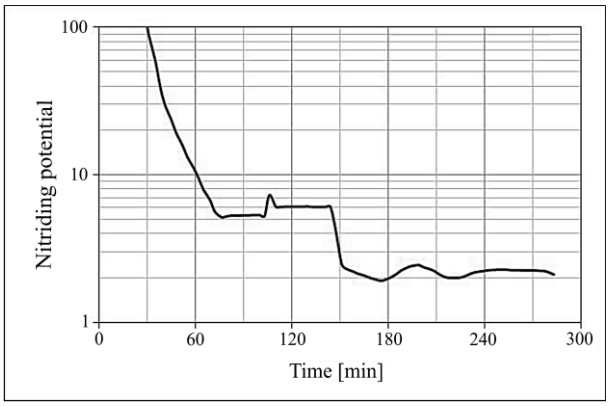

Fig. 1. Nitriding potential during gas nitriding vs. time of process

After the nitriding process, laser heat treatment was performed using TRUMPF TLF 2600 Turbo CO_2 laser system with a nominal power of 2.6 kW. The laser tracks were arranged as simple tracks. The method of single tracks' producing was shown in **Figure 2**. The surface was re-melted by the laser beam. TEM_{01^*} multiple mode of the laser beam was applied. The laser processing parameters were as follows: scanning rate v_l = 2.88 m/min and the various laser power beam (P) 0.39 kW, 0.52 kW, 0.65 kW, 0.78 kW, 0.91 kW, 1.04 kW. The laser beam diameter was equal to 2 mm. Hence, the averaging irradiance (E) ranged from 12.41 to 31.10 kW/cm^2. The focusing mirror was characterized by: curvature 250 mm, diameter 48 mm and focal length 125 mm.

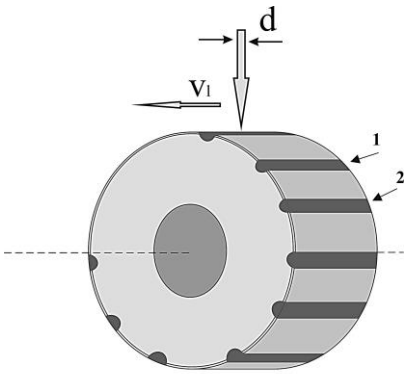

Fig. 2. The method of single tracks' producing; d – laser beam diameter (d = 2 mm); v_l – scanning rate; 1,2,...- single track

The microstructure was observed on polished and etched cross-section of the specimen using scanning electron microscope (SEM) Tescan Vega 5135. The sample were cut out perpendicular to the nitrided and laser-heat treated surface to reveal the microstructure and dimensions of the single laser tracks. Sample was etched by a reagent, consisting of 5 % nital.

Microhardness profiles, through the produced layer, were measured on polished cross-section of specimens. The Vickers method was applied for microhardness measurements with the use of the apparatus ZWICK 3212 B and Buehler Micromet II. The load of 0.05 or 0.1 kgf (0.49 N or 0.98 N) was used.

3. RESULTS AND DISCUSSION

The microstructure of 42CrMo4 steel after the controlled nitriding process was shown in **Figure 3**. The compound zone with iron nitrides consisted of a surface zone (1) and a diffusion zone (2). The gas-nitriding process resulted in a formation of a porous compound layer with a phase composition: ε + γ' [18]. In the surface zone (1) two regions were visible. The first region contained a porous ε nitrides (1a), occurring at the surface. The second compact region (1b), below this porous zone, contained ε+γ' nitrides. The thickness of the whole compound zone (1) was about 20 μm, and the thickness of the porous ε zone (1a) was equal to 8 μm. The diffusion zone (2) consisted of nitric sorbite with precipitates of γ' nitrides.

Laser modification with re-melting influenced the microstructure of nitrided layer. SE images of single laser tracks were shown in **Figure 4**. In the microstructure, four zones were visible: 1 - re-melted zone (MZ), 2 - heat-affected zone (HAZ), 3 - nitrided layer without visible effects of laser treatment and 4 - the substrate. In all laser tracks, re-melted and heat-affected zones were easily identified. The detailed analysis of the microstructure indicated that MZ consisted of

coarse martensite. The microstructure of the HAZ consisted mainly of fine-grained martensite. Below HAZ, the microstructure of diffusion zone (nitric sorbite with precipitates of γ' phase) was clearly visible. Sorbite was characteristic of the base material (4).

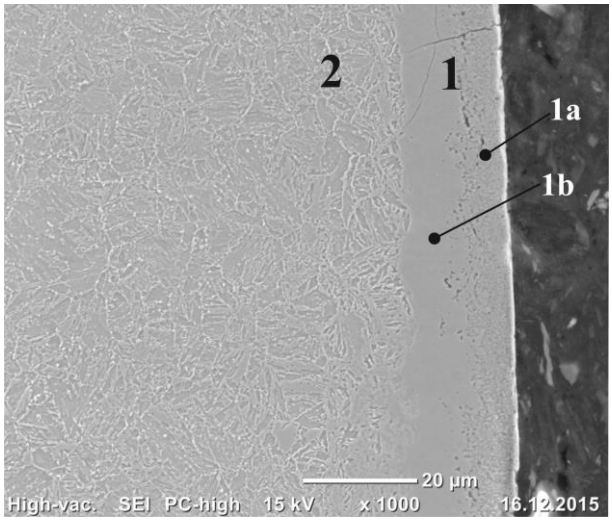

Fig. 3. Microstructure of the 42CrMo4 steel after controlled gas nitriding process; 1- compound zone; 2- diffusion zone

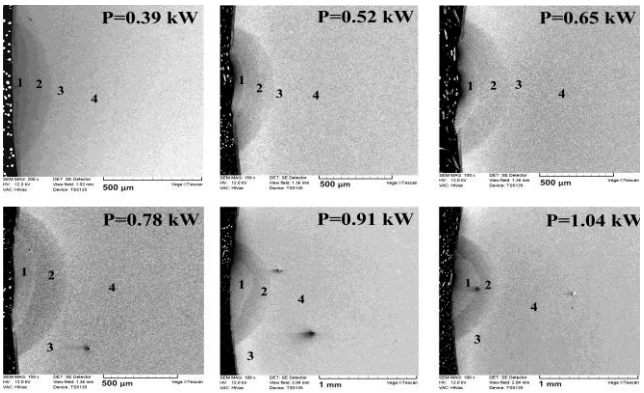

Fig. 4. Microstructure of single laser tracks produced on nitrided 42CrMo4 steel; 1- re-melted zone (MZ), 2- heat affected zone (HAZ), 3- nitrided layer without visible effects of LHT, 4- substrate

The higher laser beam power was accompanied by an increase in widths and depths of laser tracks, and more accurately: depth and widths of MZ and HAZ. The greater size of the tracks was obtained by using higher power of the laser beam. At the laser beam power above 0.78 kW, the depth of HAZ exceeded the depth of diffusion zone. The method of width and depth measurements was shown in **Figure 5a**. The influence of laser beam power on the tracks' dimensions at constant scanning rate v_l = 2.88 m/min was presented in **Figure 5b**. Depth of MZ ranged from 40 µm to 250 µm, whereas depth of HAZ varied between 200 µm and 450 µm, depending on laser beam power. There could be observed a significant increase in the depth of MZ (up to six times), caused by growth in laser beam power. MZ width increased twice, obtaining 400 µm at laser beam power 0.39 kW, and 800 µm at P = 1.04 kW. The width of HAZ increased from 800 µm to about 1200 µm within the same range of laser beam power. **Table 1** showed the results of measurements of dimensions of the single tracks and corresponding hardness.

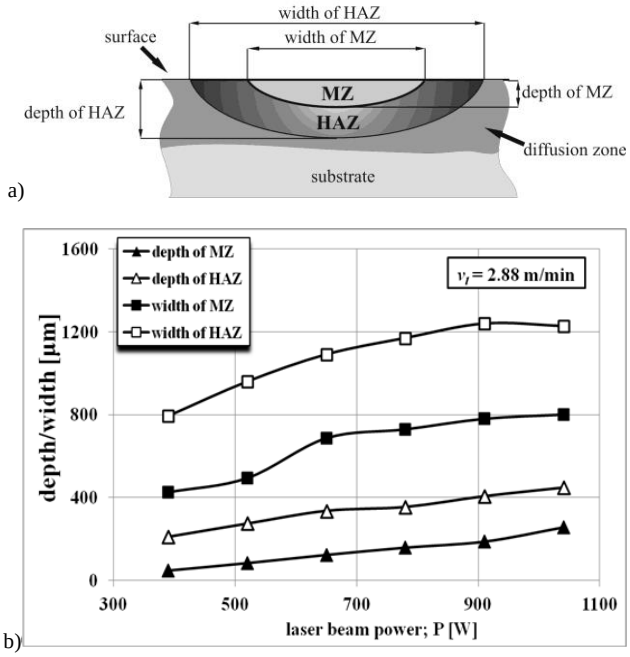

Fig. 5. Dimensions of simple laser tracks; a) method of measurement; b) influence of laser beam power P on the depths and widths of single laser tracks

The microhardness profiles of the produced layers were presented in **Figure 6**. The measurements were carried out perpendicular to the nitrided layer and to the laser tracks arranged during laser re-melting. The maximal hardness of the gas-nitrided 42CrMo4 steel was obtained in compound zone (670 HV). Next, the gradual decrease in hardness was observed.

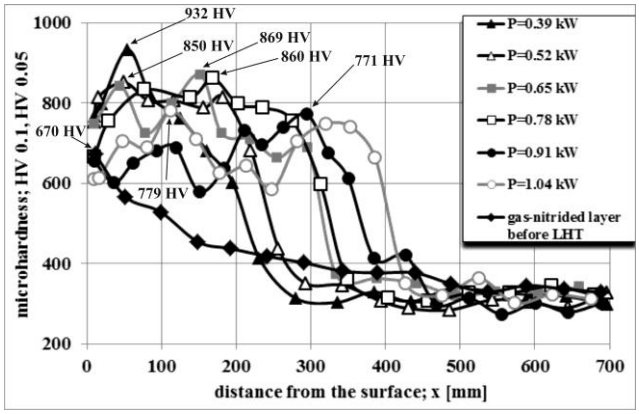

Fig. 6. Microhardness profiles of the produced simple laser tracks

The end of the diffusion zone corresponded to the depth of 300 μm. The toughened substrate had a hardness of about 330 HV. The hardness increased significantly after laser re-melting of gas-nitrided steel. Laser beam power influenced the depth of MZ and HAZ, and so the thickness of hardened zone. The greater laser beam power, the larger hardened zone. The highest microhardness was measured in MZ. Next, the gradual decrease in hardness was observed in HAZ. Outside of this zone, the hardness corresponded to toughened substrate. In order to get better characterization of hardness profiles, the measurements at the depth of 10 μm as well as maximal hardnes of MZ were analyzed. The first hardness measurements were carried out 10 μm from the surface (**Table 1**). At the laser beam power within the range of 0.39-0.65 kW, this hardness was equal to about 746-766 HV. The increase in laser beam power to 0.78-0.91 kW caused the decrease in hardness to 655-666 HV at the depth of 10 μm.

Table 1
Measurements of the width and depth of single tracks and hardness at a distance of 10 μm from the surface and the maximal hardness in re-melted zone

P [kW]	HV-distance 10 μm from the surface	HV max	MZ [μm]		HAZ [μm]	
			depth	width	depth	width
0.39	766	932	46.9	423.2	209.3	792.3
0.52	753	850	83.1	492.3	273.6	959.2
0.65	746	869	122.7	685.5	335.4	1090.7
0.78	666	860	158.3	728.5	354.2	1169.8
0.91	655	771	187.3	779.5	406.5	1239.6
1.04	608	779	256.7	799.5	448.1	1227.5

The minimal hardness at this depth (608 HV) corresponded to the laser track produced at laser beam power of 1.04 kW. The greater the power of the laser beam, the lower hardness at the surface. The maximal hardness, measured in MZ, was also determined (**Table 1**). The highest hardness of MZ (932 HV) was obtained by producing a single tracks at the laser beam power of 0.39 kW. This maximal hardness of MZ was reduced to 850-869 HV after LHT with laser beam power ranging from 0.52 to 0.78 kW. The highest laser beam powers (0.91 and 1.04 kW) resulted in further decrease in maximal hardness of MZ, obtaining 771-779 HV. The influence of laser beam power on the maximal hardness of MZ and hardness at the depth of 10 μm was presented in **Figure 7**.

The increased microhardness after LHT was caused by a changed microstructure, especially by the presence of martensite in hardened layer (MZ and HAZ). Additionally, nitrogen, dissolved in austenite during re-melting, caused increase in hardenability. The diminished hardness close to the surface (at depth of 10 μm) could result from the lower cooling rate in this area. In HAZ, microhardness decreased gradually due to reducing the percentage of martensite within the distance from the surface.

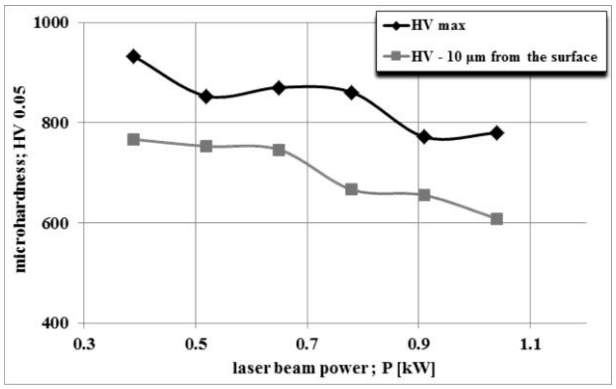

Fig. 7. Maximal hardness of MZ and hardness in the distance of 10 μm from the surface vs. laser beam power

Next hardness obtained the values characteristic of the base material, i.e. toughened 42CrMo4 steel. At the laser beam power of 0.39 or 0.52 kW, the significant reduction of hardness was observed at the end of HAZ, comparing to the nitrided layer. It could be caused by the higher temperature in this region during LHT, comparing to the temperature of tempering before nitriding.

4. CONCLUSIONS

Modification by re-melting using different laser beam powers was proposed to change microstructure and to improve hardness of gas-nitrided layer produced on 42CrMo4 steel. The controlled gas nitriding process was carried out at 570°C for 4 h on toughened steel using changeable nitriding potential in order to limit the thickness of compound zone. The nitrided layer was composed of this compound zone, including ε and γ' nitrides, and diffusion zone (nitric sorbite with γ' precipitates). The thickness of the nitride zone was above 20 μm, and the porous zone (close to the surface) was 8 μm thick. The maximal hardness of the nitrided layer was measured in compound zone and was equal to 670 HV, gradually decreasing to about 330 HV in the toughened substrate.

Laser re-melting changed the microstructure of previously nitrided layer. The microstructure of laser heat-treated nitrided steel consisted of four zones: 1- re-melted zone (MZ), 2- heat-affected zone (HAZ), 3- nitrided layer without visible effects of laser treatment and 4- the substrate. LHT caused an increase in hardness of the nitrided layer because of the formation of martensite in MZ and, partially, in HAZ. Additionally, laser re-melting resulted in dissolving the iron nitrides in austenite. This was the reason for increase in hardenability. The larger hardened zone was also observed after laser modification using laser beam power above 0.78 kW. However, it corresponded to the diminished hardness close to the surface. The maximal surface hardness was observed at laser beam powers within the range from 0.39 to 0.65 kW. Therefore, re-melting at these laser processing parameters seemed to be most advantageous.

REFERENCES

[1] **Altinsoy I, Onder K.G, Celebi Efe F.G, Bindal C.**, Gas nitriding behaviour of 34CrAlNi7 nitriding steel, Acta Physica Polonica A 2014, vol.125, s. 414-416.

[2] **Małdziński L, Tacikowski J.**, ZeroFlow gas nitriding of steels. In: Mittemeijer EJ, Somers MAJ, editors. Thermochemical Surface Engineering of Steels Improving Materials Performance, Woodhead Publishing Series in Metals and Surface Engineering, Elsevier, 2015, vol. 62, s. 459-483.

[3] **Michalski J., Tacikowski J., Wach P., Ratajski J.**, Controlled gas nitriding of 40 HM and 38 HMJ steel grades with and without the surface compound layer, composed of iron nitrides. Maintenance Problems, 2006, vol. 2, s. 43-52.

[4] **Michalski J., Tacikowski J., Wach P., Lunarska E., Baum H.**, Formation of single-phase layer of γ'-nitride in controlled gas nitriding. Metal Science and Heat Treatment, 2005, vol. 47, s. 516÷519.

[5] **Fu H., Zhang J., Huang J., Lian Y., Zhang C.,** Effect of temperature on microstructure, corrosion resistance, and tougness of salt bath nitrided tool steel, Journal of Materials Engineering and Performance, 2016, vol. 25, s. 3-8.

[6] **Chen J.S., Yu C., Lu H.**, Phase stability, magnetism, elastic properties and hardness of binary iron nitrides from first principles, Journal of Alloys and Compounds, 2015, vol. 625, s. 224-230.

[7] **Taktak S., Gunes I.,** Effect of pulse plasma nitriding on tribological properties of AISI 52100 and 440C steels, Journal Surface science and Enigineering, 2014, vol. 8, no. 1, s 39-56.

[8] **Carpene E., Schaaf P.,** Laser nitriding of iron and aluminum**,** Applied Surface Science, 2002, vol. 186, s. 100-104.

[9] **Chang K.M., Kuo C.C., Chang Y.W., Chao C.G., Liu T.F.**, Effects of gas nitriding pressure on the formation of nanocrystaline AlN in plasma nitrided Fe-9Al-28Mn-1.8C alloy, Surface & Coatings Technology, 2015, vol. 254, s. 313-318.

[10] **Li S., Hu S., Hee A.C., Zhao Y.**, Surface modyfication of a Ti2AlC soft ceramic by plasma nitriding treatment, Surface & Coatings Technology, 2015, vol. 281, s. 164-168.

[11] **Yan M.F., Wang Y.X., Chen X.T., Guo L.X., Zhang C.S., You Y., Bai B., Chen L., Long Z., Li R.W.,** Laser quenching of plasma nitrided 30CrMnSiA steel, Materials and Design, 2014, vol. 58, s. 154–160.

[12] **Colombini E., Sola R., Parigi G., Veronesi P., Poli G.**, Laser Quenching of Ionic Nitrided Steel: Effect of Process Parameters on Microstructure and Optimization, Metallurgical and materials transactions A, 2014, vol. 45A, s. 5562-5573.

[13] **Li Y., Wang L., Shen L., Zhang D., Wang C.**, Plasma nitriding of 42CrMo low alloy steels at anodic or cathodic potentials, Surface & Coatings Technology, 2010, vol. 204, s. 2337-2342.

[14] **Wang L., Li Y., Wu X.**, Plasma nitriding of low alloy steels at floating and cathodic potentials, Applied Surface Science, 2008, 254, s. 6595-6600.

[15] **Roliński E.**, Plasma-assisted nitriding and nitrocarburizing of steel and other ferrous alloys, In: Mittemeijer EJ, Somers MAJ, editors. Thermochemical Surface Engineering of Steels Improving Materials Performance, Woodhead Publishing Series in Metals and Surface Engineering, 2015, no. 62, s. 413–457.

[16] **El-Hossary F.M., Negm N.Z., Abd El-Rahman A.M., Raaif M., Seleem A.A., Abd El-Moula A.A.**, Tribo-mechanical and electromechanical properties of plasma nitriding titanium, Surface & Coatings Technology 2015, no. 276, s. 658-667.

[17] **She D., Yue W., Fu Z., Wang C., Yang X., Liu J.**, Effects of nitriding temperature on microstructures and vacuum tribological properties of plasma-nitrided titanium, Surface & Coatings Technology 2015, no. 264, s. 32-40.

[18] **Kulka M., Michalski J., Panfil D., Wach P.**, Laser heat treatment of gas-nitrided layer produced on 42CrMo4 steel, Inżynieria Materiałowa 5(207) (2015) 301-305.